LITHIUM-DOPED NICKEL OXIDE GROWN BY DIFFERENT PVD METHODS FOR HOLE-SELECTIVE CONTACTS IN SILICON-BASED HETEROJUNCTIONS

F. Menchini[1], S. Rakhshani[1], L. Serenelli[1], L. Martini[1], E.Salza[1], P. Mangiapane[1], M. Izzi[1], A. Latini[2], M. Tucci[1]
[1]ENEA, TERIN Department, via Anguillarese 301, 00123 Roma, Italy
[2]Sapenza University, Chemistry Department, Roma, Italy

ABSTRACT: Carrier-selective contacts are well known to be one of the keys to obtain cost effective high-efficiency solar cells. In silicon-based heterojunctions the contacts are usually obtained by doped hydrogenated amorphous-silicon (a-Si:H) layers, which however introduce important absorption losses and require expensive production processes. Many candidate materials have been identified to substitute a-Si:H layers, but their full exploitation is frequently limited by the constrain of being resistant to thermal treatments up to at least 250°C. Among them, doped nickel oxide seems to be ideal to form a hole-selective contact thanks to the alignment of its valence band with that of silicon. In this work we grew films of lithium-doped nickel oxide (NiOx:Li) by different PVD techniques and tested their behavior in hole-selective contacts in silicon heterojunctions. The J-V characteristics of the proof-of-concept devices demonstrate the possibility to replace p-type a-Si:H film with NiOx:Li, although further improvements are needed to optimize the performances and solve the issue related to silicon lifetime degradation.
Keywords: selective contact, nickel oxide, heterojunction

1 INTRODUCTION

In the first half of years 2010s the historical power conversion efficiency record for crystalline silicon solar cells, held by UNSW, was reached and overcome by Panasonic amorphous silicon/crystalline silicon heterojunctions (HJs) [1]. This finally established the potential of HJ technology, which currently still hits records by different PV players. At the time of writing this work LONGI settled an efficiency of 27.6%, which is close to the theoretical limit of 29.43% [2, 3].

The main keys to the HJ success are the silicon surface passivation with very thin hydrogenated amorphous-silicon (a-Si:H) layers and the carrier-selective contacts, as obtained by doped a-Si:H layers, which are able to induce the inversion layer (p) and then the p-n junction inside the n-doped crystalline silicon (n-c-Si) absorber and to form an effective selective base contact able to collect the electrons and repulse the holes by simply using the band alignment mismatch at the a-Si:H/c-Si interface. Indeed, if the p-n junction is fully formed within the high-lifetime silicon bulk, the SHR recombination at midgap when the Fermi level crosses the p-n junction is strongly reduced, thus resulting in excellent open-circuit voltages. However, such doped a-Si:H layers are at the same time the limit of HJ cells, because they introduce important absorption losses and require expensive production processes due to the toxic gases needed for their doping. These drawbacks have recently urged researchers to test new alternative materials to be introduced in the hole- and electron-selective stacks as carrier-selective contacts [4]. Many candidates have been identified to substitute a-Si:H and successfully employed [5]. Among them, nickel oxide (NiOx) is theoretically characterized by a good alignment of its valence band with that of silicon, which confers it optimal characteristics as hole-extracting layer as confirmed by theoretical calculations [6]. On the other side, a doping of NiOx is needed in order to push its Fermi level close to the valence band and induce a deep inversion layer in the n-type doped c-Si [7]. Nevertheless, other calculations [8] illustrated that, due to the interactions of NiOx with a-Si:H, a thin SiOx layer could be formed, which could worsen the transport properties also because of a valence band energy modulation. Then it was shown that it is necessary to greatly increase the NiOx doping to enhance the carrier selectivity. Nonetheless, only a few experimental results have been presented on the topic yet [9, 10].

One of the crucial parameters to obtain working devices is the defect density at the c-Si/NiOx interface. A simulation contained in [11] evidenced that a defect density below 2×10^{10} cm^{-2} is needed to avoid undesirable barriers against carrier collection. These findings establish the necessity of a good passivation of the c-Si surface to improve the V_{OC}. Once the surface passivation is ensured, doping is the main parameter to adjust. Different elements (not only monovalent) can be used as dopants for NiOx, among which Li^+ is recommended for the purpose due to its ionic radius (0.135 Å) which is very similar to that of Ni^{2+} (0.145 Å).

In this work we illustrate the application of lithium-doped nickel oxide, at various concentrations, to the aim of obtaining a hole selective contact for n-type silicon. In order to avoid sputtering damages, we chose a PVD approach, employing e-beam and thermal evaporation. The material was initially characterized by its optical and electrical properties, and then used as emitter in HJ devices production on n-type c-Si wafers.

2 EXPERIMENTAL

We deposited films of lithium-doped nickel oxide (NiOx:Li) starting from calcined precursors containing different dopant concentrations. Firstly, $Ni(NO_3)_2{\cdot}6H_2O$ was calcinated at 800°C to obtain NiOx. Then, to obtain the NiOx:Li doped samples, the proper amount of $Li(NO)_3$ was added to NiOx, pressed in a pellet and heated up to 1000°C for 3 hours. Two doping concentrations were considered, 3% and 5% at.

E-beam evaporation was conducted in a Balzer system at room temperature, with a deposition rate of 0.1 nm/sec, a base pressure of 6-8$\times10^{-6}$ mbar and an accelerating voltage of the electron gun of 3.5 kV. The substrates, positioned on a rotating carrier, were not intentionally heated during the deposition. The thickness of the films was controlled by a quartz oscillator during the growth process.

Thermal evaporation was obtained by heating the precursors in an alumina crucible inserted in a tungsten heater with 0.1-0.2 Å/s deposition rate at a 5×10^{-6} mbar base pressure.

The films, deposited on soda lime glasses, were optically characterized with the aid of a Perkin Elmer Lambda 950 spectrophotometer, measuring reflectance and transmittance and extracting the optical gap (Eg) from the Tauc plot. The dopant activation energy was calculated by current measurements at various temperatures in a cryogenic system.

In order to test the performances of the NiOx:Li films inside a device, n-type 1-5 Ω·cm textured c-Si wafers were used as substrates, which were passivated on both sides by a 5.5 nm-thick layer of amorphous hydrogenated silicon oxide (a-SiOx:H) deposited via PECVD [12]. This latter material equals the good passivation properties of amorphous silicon, but with an enhanced Eg that favours short-wavelength light absorption. Different NiOx:Li layers were deposited on one side of the c-Si substrates and then covered by an 80 nm-thick layer of Indium Tin Oxide (ITO) to form the emitter contact. The base contact was fabricated in two ways: one set of samples had an unpassivated ohmic contact obtained by means of a thick film of InGa eutectic, the other one contained a 18 nm-thick layer of n-type a-Si:H covered by an 80 nm-thick layer of ITO and a full metal contact of screen printed Ag, subsequently annealed at 180°C for 10 minutes to improve TCO lateral conductivity and transparency and recover sputtering damage.

Selected samples were characterised by Glow Discharge Optical Emission Spectroscopy (GDOES) in a Horiba Jobin Yvon GD Profiler 2 spectrometer. This technique provides an in-depth chemical composition of the film by etching the sample with an Ar plasma and analysing the plasma radiation emitted from the etched material, which wavelength can be correlated to the excited element. The spectra show the signal variation for each element vs the etching time, which is proportional to the etched thickness of material. The devices were characterized by light AM1.5G and dark current density-voltage (J-V) measurements, as well as by external quantum efficiency (EQE) measurements.

3 RESULTS

3.1 Optical characterization

The e-beam evaporated NiOx:Li films deposited on glass, undoped and with 3% and 5% doping, were optically characterized. The absorption coefficient (α) comparison, shown in Fig. 1A, evidences some differences introduced by the doping atoms influencing the microstructural properties of material, and in turn their optical properties. It is expected that by increasing the Li doping concentration the absorption increases [13], however, no clear trend was observed in this case. It is interesting to notice the difference between absorption coefficients of the various Ni oxides, both doped and undoped, and the p-type doped a-Si:H, reported in the same graph as a grey dashed line, confirming the higher transparency of NiOx:Li with respect to the amorphous silicon counterpart. Then the band gap energy (Eg) of the material was extrapolated from the Tauc plot shown in Fig. 1B. The bandgap of all films is around 3.7 eV, with a slightly higher value for the doped films, in accordance with other literature values [14, 15].

3.2 Electrical characterization

In order to estimate the lateral conductivity of the films, two ITO pads were deposited on the samples to ensure the contact, which was proven to be ohmic, and a current-voltage (I-V) characteristic was collected on the as-deposited sample and after a thermal annealing at 180°C for 30 minutes. The results are reported in Fig. 2A as a function of Li doping.

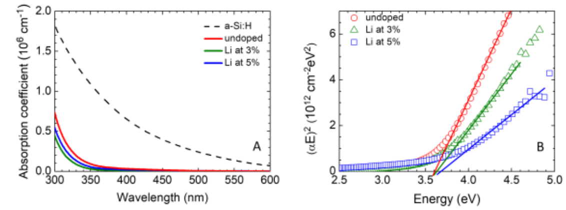

Figure 1: Optical characterization of NiOx:Li films with Li doping at 0% (undoped), 3% and 5% at. concentrations. A: absorption coefficient, B: Tauc plots for the same NiOx film as in A, with the extrapolation of the linear part indicating the Eg. In Fig. 1A the absorption coefficient of a-Si:H is reported for comparison

Figure 2B reports the trend of the activation energy as a function of Li doping as evaluated from I-V measurements as a function of temperature.

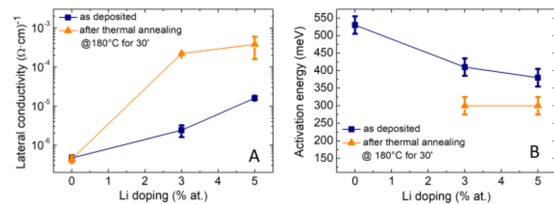

Figure 2: A: lateral conductivity and B: activation energy of NiOx:Li films with different Li doping before (blue square symbols) and after (orange triangle symbols) a thermal annealing treatment of 180°C for 30'

As the Li doping increases the conductivity of the films increases from 4.7×10^{-7} $(\Omega\cdot cm)^{-1}$ in the undoped sample to 1.8×10^{-3} $(\Omega\cdot cm)^{-1}$ in the highly-doped sample, while in the same range of Li doping the activation energy drops from 530 mV to 140 mV. Both results are in accordance with the increase of doping: an increased concentration of Li in the material induces the substitution of more Ni^{2+} lattice cations, forming valence vacancies, i.e. free holes that increase the p-type conductivity of the material. The activation energy is consequently reduced because of the approaching of the Fermi level to the valence band. After thermal annealing the conductivity of the samples increase, and the activation energy consequently reduces. The lower the activation energy value is, the more the Fermi level of NiOx:Li is shifted towards the valence band edge, and a better band alignment is achieved. Thus, a compromise between doping concentration and activation energy and usage of a buffer layer with lower Eg can be investigated.

3.3 Devices

3.3.1 E-beam evaporation

Based on these premises, several devices were fabricated in order to test the performances of the NiOx:Li films as hole extractors, as illustrated in the experimental section. 20 nm-thick films were deposited on passivated c-Si substrates contacted by a-Si:H and ITO con the back

10.4229/EUPVSEC2023/1CV.3.28

side, as described in the Experimental section and depicted inside Fig. 3A. The light and dark J-V characteristics and external quantum efficiency of the samples were measured, and the best results, corresponding to the sample containing a Li doping of 5% at., are shown in Fig. 3.

The J-V characteristic (Fig. 3A) shows a V_{OC} of 324 mV, a FF of 37.1% and a Jsc of 35.4 mA/cm^2, confirmed by the external quantum efficiency reported in Fig. 3B. The fact that the light and dark characteristics do not cross each other (lower inset in Fig. 3A) is an indication that no V_{OC} drop due to a valence band offset is present in the cell, as explained in [16].

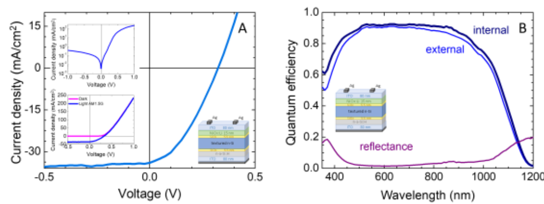

Figure 3: A: light and dark (upper inset) J-V characteristics and B: quantum efficiency of the best performing cell, containing a NiOx:Li film with Li at 5% at. The lower inset in A shows the superposition of dark and light characteristics, showing that the two curves do not cross each other

However, the overall features of the cell are still scarce. Besides the non-optimised front and back contacts and thickness of the NiOx:Li film, the main reason for the low performances of the cell was connected to the low value of the V_{OC}; this was certainly limited due to small area of the cells (which were obtained by cleaving larger wafer [17]) and by the very low lifetime of the structure. In fact the initial lifetime of the passivated substrate (above 1 ms) was strongly deteriorated after the NiOx:Li film deposition, when it reached 100 µs, and not even the thermal treatment was able to restore it. We theorised that this could be a consequence of the e-beam deposition technique, during which x-rays are emitted from the electronic gun [18].

To conclude, the exposed experiments constitute a proof-of-concept for Si-based HJ cell containing a NiOx:Li hole selective layer, which shows that the material is well suited for such application and could be even further optimised in terms of doping. However, the e-beam deposition technique turned out not to be suitable for depositing materials over passivated c-Si substrates, because of the remarkable and permanent damages to the passivation, which leaded to very low V_{OC} values.

3.3.2 Thermal evaporation

To overcome this problem, we explored the possibility to deposit the NiOx:Li films by thermal evaporation. The technique does not imply any emission of radiation, but presents some complications due to the high evaporation temperatures of the source material: in particular, NiOx has a fusion temperature of around 2000°C. The evaporation material was constituted by the same pellets already used for e-beam evaporation, while different evaporation crucibles were tested. Indeed, not all the crucible materials could be suitable to sustain high electrical power to ensure the high temperature needed to evaporate the pellets. At the same time, it is difficult to find a material for crucible which, once heated at such high temperatures, does not evaporate itself, thus contaminating the deposited film. A cylindrical alumina crucible was chosen due to its high temperature resistance, and was inserted in a tungsten heater. The deposition rate was kept very low to avoid excessive thermal stress. Starting from the best results obtained from e-beam deposition, we deposited 10 nm-thick 5%-doped NiOx:Li films over a passivated c-Si substrate contacted on the back by InGa, as described in the Experimental section and reported in the scheme in Fig. 4B. The light J-V characteristics of the sample are reported in Fig. 4A and show a typical p-n junction behaviour. The relatively high Jsc of 32.3 mA/cm^2 confirms the high transparency of the window layer, and the FF (nearly 55%) higher than the previously reported ones confirms the effectiveness of the doping. The cell behaviour is compromised mostly in terms of V_{OC} (335 mV), which is anyway slightly higher than that of the corresponding cell obtained by e-beam evaporation: the latter one had also the back side passivated, while in this case the ohmic back contact is simply made by InGa, as evident from the EQE in Fig. 4B. The dark characteristic (inset in Fig. 4A) shows a high recombination behaviour evident from the high current density in reverse bias and low forward bias conditions. The initial lifetime of the passivated substrate of 1.5 ms dropped to a few tens of µs after the deposition of the emitter, and could not be recovered after the thermal annealing. In this case, even if the damaging x-rays connected to e-beam evaporation was no more an issue, some other source of damage for the passivation should have been present. Probably a diffusion of some metal may have happened during deposition, coming from the heater-crucible system, as they were heated at very high temperatures.

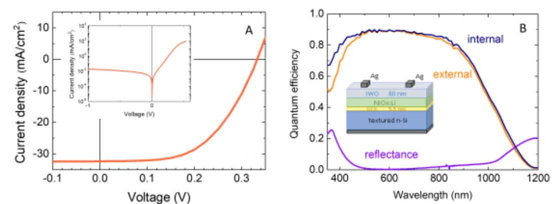

Figure 4: A: light and dark (inset) J-V characteristics and B: quantum efficiency of a cell containing a thermally-evaporated NiOx:Li film with 5% at. Li doping

To check this hypothesis the sample was examined with the aid of GDOES, and the results are shown in Fig. 5. In the first part of the profile, besides the expected signals form Ni and Li (and O), also a contribution from Al is clearly visible, revealing that a metallic contamination is coming from the alumina crucible (we previously checked that this contamination was not present in the pellets). The metal contamination is also suggested by the unexpectedly high conductivity of the sample (around 10^{-2} Ω·cm), which is many orders of magnitude higher than the corresponding value found for the e-beam evaporated sample (Fig. 2B). Obviously, these contaminations are not acceptable, as they are completely uncontrolled, especially after a thermal treatment, so they must be avoided a priori. Moreover, they could also be at the basis of the unexpected damage of the substrate after deposition.

Thus, since NiOx:Li appears to be a promising candidate to form a hole selective contact to silicon, an

alternative deposition method should be found. A viable hypothesis could be the evaporation of metallic nickel in oxygen atmosphere to form NiOx. In this case the doping could be obtained by co-evaporating a source containing the doping element.

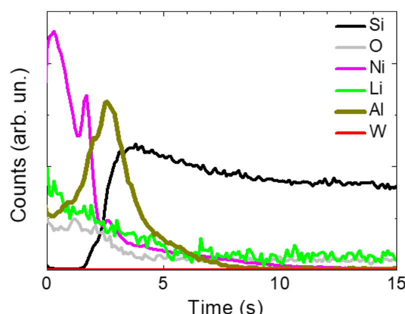

Figure 5: GDOES profiles of NiOx:Li films deposited on a c-Si/a-SiOx:H substrate by thermal evaporation from an alumina crucible in a W heater.

4 CONCLUSIONS

NiOx is a promising material to form an emitter on HJ solar cells on n-type doped c-Si wafer. However, there is the necessity of a strong doping in order to obtain good results. Li was used to dope NiOx and conductivity values of 10^{-4} $(\Omega\cdot cm)^{-1}$ and activation energies around 300 mV were measured. The introduction of a passivating layer allowed the production of working devices, even with low performances and efficiencies around 5%, mainly connected to the evaporation techniques of the ceramic NiOx:Li precursors. In particular, the e-beam evaporation technique was demonstrated not to be compatible with passivated substrates, due to the unavoidable damage caused by x-rays. The more versatile thermal evaporation technique was also tested, but after many and different attempts it was found out that the used NiOx:Li sintered precursor required too much power to be evaporated, thus causing contaminations coming from the crucible. The reduced lifetimes after deposition suggested both a damage induced by diffused species and a band misalignment due to low NiOx:Li doping. However, the material continues being interesting, so that the challenge for its optimisation still remains open. Thus, since the evaporation from a ceramic precursor seems to produce inevitable drawbacks, an alternative approach could be the co-evaporation of metallic nickel and dopant precursor in oxygen atmosphere, which could reduce the necessity for high temperatures.

5 ACKNOWLEDGEMENT

This work was funded under the National Recovery and Resilience Plan (NRRP), Mission 4 Component 2 Investment 1.3 - Call for tender No. 1561 of 11.10.2022 of Ministero dell'Università e della Ricerca (MUR); funded by the European Union – NextGenerationEU. Project code PE0000021, CUP I83C22001800006, Project title "Network 4 Energy Sustainable Transition – NEST" and by the Italian Ministry of Environment and Energy Security in the framework of the Operating Agreement with ENEA for Research on the Electric System.

6 REFERENCES

[1] https://www.nrel.gov/pv/cell-efficiency.html, 2023.
[2] M.A. Green, E.D. Dunlop, G. Siefer, et al. Solar cell efficiency tables (Version 61), Progress in Photovoltaics: Research and Applications 31:1 (2023) 3-16
[3] A. Richter, M. Hermle, S.W. Glunz, IEEE Journal of Photovoltaics 3:4 (2013) 1184-1191
[4] J. Bullock, M. Hettick, J. Geissbühler, et al., Nature Energy 1 (2016) 15031
[5] Y. Wang, S. T. Zhang, L. Li, et al., EcoMat 5:2 (2022) e12292
[6] R. Islam and K. C. Saraswat, Proceedings IEEE 40th Photovoltaics Specialists Conference PVSC, 2014, pp. 285-289
[7] H. Imran, T. M. Abdolkader, IEEE Transactions in Electron Devices 63:9 (2016) 3584-3590
[8] M. Boccard, R. Woods-Robinson, A. Fioretti, et al., Proceedings of the 37th EU PVSEC 2020, online, 2BO.3.3, 21 pages
[9] H. Hsu, N. F. Wang, Y. Z. Tsai, et al., Thin Solid Films 573 (2014) 159-163
[10] X. Yang, W. Liu, J. Chen, et al., Applied Physics Letters 112 (2018) 173904
[11] F. Menchini, M. L. Grilli, T. Dikonimos, et al., Physica Status Solidi C 13:10-12 (2016) 1006-1010
[12] L. Serenelli, L. Martini, L. Imbimbo et al., Applied Surface Science 392 (2017) 430-440
[13] W. Chia-Ching, Y. Cheng-Fu, Nanoscale Research Letters 8:1 (2013) 33
[14] J. Arunodaya and T. Sahoo, Materials Research Express 7 (2020) 016405
[15] D. Paul Joseph, M. Saravanan, B. Muthuraaman, et al., Nanotechnology 19 (2008) 485707
[16] L. Serenelli, L. Martini, F. Menchini, et al., Progress in Photovoltaics: Research and Applications 29:7 (2021) 876-884
[17] L. Serenelli, L. Martini, F. Menchini, et al., Solar Energy 258 (2023) 2-7
[18] T. Rahman, A. To, M.E. Pollard, et al., Progress in Photovoltaics: Research and Applications 23 (2018) 38-47